Magn Reson Mater Phy (2013) 26:291–301
DOI 10.1007/s10334-012-0355-2

RESEARCH ARTICLE

Magnetization transfer for the assessment of bowel fibrosis in patients with Crohn's disease: initial experience

Shila Pazahr · Iris Blume · Pascal Frei · Natalie Chuck · Daniel Nanz · Gerhard Rogler · Michael Patak · Andreas Boss

Received: 26 May 2012 / Revised: 26 August 2012 / Accepted: 22 October 2012 / Published online: 9 November 2012

Abstract
Object To assess the feasibility of magnetization transfer (MT) imaging of the bowel wall in patients with Crohn's disease (CD), and to evaluate its utility for the detection of intestinal fibrosis.
Materials and methods In this prospective study, 31 patients (age 39.0 ± 13.2 years) with CD were examined in a 1.5T MR scanner. To establish a standard of reference, two independent readers classified the patients in different disease states using standard MR enterography, available clinical data and histological findings. In addition to the standard protocol, a 2D gradient-echo sequence (TR/TE 32 ms/2.17 ms; flip angle 25°) with/without 1,100 Hz off-resonance prepulse was applied. MT ratios (MTR) of the small bowel wall were computed off-line on a pixel-by-pixel basis.
Results The MT sequences acquired images of sufficient quality and spatial resolution for the evaluation of the small bowel wall without detrimental motion artefacts. In normal bowel wall segments, an intermediate MTR of 25.4 ± 3.4 % was measured. The MTR was significantly increased in bowel wall segments with fibrotic scarring (35.3 ± 4.0 %, $p < 0.0001$). In segments with acute inflammation, the mean MTR was slightly smaller (22.9 ± 2.2 %).
Conclusion MT imaging of the small bowel wall is feasible in humans with sufficient image quality and may help with the identification of fibrotic scarring in patients with CD.

Keywords Magnetization transfer contrast imaging · Crohn disease · Fibrosis

S. Pazahr (✉) · I. Blume · N. Chuck · D. Nanz · M. Patak · A. Boss
Department of Diagnostic and Interventional Radiology, University Hospital Zurich, Rämistr. 100, 8091 Zurich, Switzerland
e-mail: shila.pazahr@usz.ch

P. Frei · G. Rogler
Department of Gastroenterology, University Hospital Zurich, Zurich, Switzerland

Introduction

Crohn's disease (CD) often exhibits a patchy pattern of bowel affection with intact bowel segments interspersed with short inflamed segments ("skip lesions"). Complications of the chronic inflammation are formation of fistulae, abscesses and intestinal strictures, associated with abdominal pain, nausea and vomiting which may lead to small bowel obstruction. A stenosis may be caused by acute inflammation leading to mucosal swelling or chronic fibrosis due to scarring. The distinction of the two aetiologies is of critical importance for the management of CD patients. Acute inflammation may well be treated with anti-inflammatory medication such as corticosteroids, or anti-bodies against tumor necrosis factor (TNF) (e.g., infliximab, adalimumab or certolizumab pegol). However, these drugs may have severe adverse effects; thus, any inappropriate application, for example, in case of fibrosis-induced stenosis needs to be avoided. The only treatment option for severe fibrotic strictures or stenoses remains surgery. A decision for surgery should not be made too late as complication rates (e.g., anastomosis leakage) are higher when an emergency situation (e.g., acute bowel obstruction) is apparent. In contrast, timely elective surgery based on reliable imaging would have the best outcome.

Standard MR enterography (MRE) protocols for the evaluation of small bowel structures include steady state

free precession sequences, T2-weighted fast spin-echo sequences and spoiled T1-weighted 3D encoded gradient-echo sequences for post-contrast imaging [1]. Recently, as an additional contrast mechanism, magnetization transfer (MT) was proposed for detection of bowel fibrosis in Crohn's disease [2]. MT imaging attempts to quantify the extent of MT between hydrogen nuclei in mobile environments, predominantly in "free" water molecules, and hydrogen nuclei in more slowly reorienting environments, predominantly covalently or non-covalently bound to macromolecules. The exchange process involves chemical exchange of protons and/or through-space dipole–dipole cross-relaxation. The MT effect grows with the number of hydrogen nuclei that switch from a high-mobility environment, such as in a free water molecule, to a low-mobility environment, such as, for example, in a hydroxyl group bound to a macromolecule. Thus, the effect size represents a rather indirect measure of the concentrations of corresponding macromolecules, for example, proteins, such as collagen, in an aqueous physiological environment. To observe and measure it, two gradient-echo data sets are typically acquired, with and without application of an off-resonant prepulse that saturates the low-mobility proton pool of hydrogen nuclei and results in a net signal loss. The relative signal intensities in the two data sets allow calculation of the MT ratio (MTR), which is characteristic for a given tissue and the chosen sequence parameters [3].

In an animal study using Lewis rats with subserosally injected peptidoglycan-polysaccharide (PG-PS) for development of bowel inflammation, Adler et al. [2] found a good correlation between the MTR and the tissue fibrosis as well as collagen content 28 days post-injection.

The aim of our study was to assess the feasibility of MT imaging of the bowel wall in patients with CD, and to evaluate its utility for the detection of intestinal fibrosis.

Materials and methods

Patients

This prospective study was approved by the local Ethics committee. All patients gave written informed consent to the MR examination as well as to the scientific evaluation of the data sets. We consecutively included 31 patients older than 18 years (10 women, 21 men; mean age 39.0 ± 13.2 years; range 18–73 years; mean BMI 22.6 ± 4.8 kg/m^2; range 14.9–34.6 kg/m^2) with known ($n = 29$) or suspected CD ($n = 2$), and an indication for a MR imaging (MRI) examination of the small bowel (Table 1). The patients were recruited and scanned between December 2010 and February 2012. Exclusion criteria were typical contraindications to MR imaging (MR incompatible metal implants, pacemakers, cochlear implants, claustrophobia, etc.).

MR scanner

All MR studies were performed on a 1.5 Tesla MRI unit (Philips Achieva, Philips Healthcare, Best, The Netherlands) using a phased-array coil with 16 anterior and 16 posterior elements. The MR scanner was equipped with Dual Quasar Gradients (slewrate 180 mT m^{-1} ms^{-1}, maximal gradient strength 33 mT/m).

Imaging protocol

Patient preparation included fasting of at least 4 h before the MR examination. 1,000 ml of oral contrast medium (2.5 % mannitol solution) was ingested by the patient over a period of 1 h prior to imaging for a better distension of the bowel lumen [4, 5]. Additionally, the patients received a water enema (400–600 ml) immediately before the procedure provided they had consented to this previously. Bowel paralysis was induced by twofold intravenous injection of 10 mg scopolamine butyl bromide (Buscopan, Böhringer Ingelheim, Biberach, Germany), the first time before the start of the imaging and the second time just before the contrast-medium application.

The individual parameters of each imaging sequence are displayed in Table 2. The imaging protocol started with gradient-echo localizers in all 3 orientations. Axial and coronal 2D-encoded single-shot T2w fast spin-echo sequences, a 2D coronal steady state free precession (SSFP) sequence, a 3D coronal and a 2D axial T1-weighted gradient-echo sequence were acquired for visualization of bowel morphology.

For MT imaging, two different imaging sequences were tested: a 3D gradient-echo sequence (4 patients; Table 1 patient 1–4) and a 2D gradient-echo sequence (27 patients; Table 1 patient 5–31). Each sequence was acquired 2 times, with and without the off-resonance MT preparation prepulse. For both sequences, the off-resonance prepulse had a Gaussian shape with a frequency offset of 1,100 Hz, a maximum effective B1 field of 15.7 μT, a duration of 1,502 μs, an effective flip angle of 620° and a bandwidth of 399 Hz. The pool of the low-mobility protons shows a fast relaxation; therefore, MT prepulses have to be applied with high frequency to achieve sufficient saturation. The shortest possible TR including a MT prepulse of 32 ms was applied in the both MT sequences. Excitation angles were chosen relatively small to keep the influence of the MT prepulse on the tissue equilibrium magnetization as large as possible.

After intravenous bolus injection of 0.1 mmol/kg body weight of Gd-DOTA (Dotarem, Guerbet, Paris, France) at an injection rate of 2 ml/s, a coronal T1-weighted

Table 1 Patients data and MTR values of the measured bowel wall

Patient	Gender	Age	Diagnosis	Clinical activity		Disease state		Main localization	Stenosis/ stricture	MTR-n (%)	MTR-p (%)	$\|\Delta\|$ difference (%)
				R1	R2	R1	R2					
1	M	37	CD	+	+	A + C	A + C	Terminal ileum	Yes	*		
2	F	23	CD	++	+	A + C	A + C	Terminal ileum	No	*		
3	M	34	IC	+	++	A + C	A + C	Sigma/rectum	Yes	*		
4	M	49	CD	++	++	C	C	Terminal ileum	No	*		
5	M	18	CD/CMV	+++	+++	A	A	Colon	Yes	N/A	20.7	/
6	M	33	CD	+	+	C	C	Terminal ileum	No	26.7	30.4	3.72
7	F	35	CD	+++	+++	A + C	A + C	Terminal ileum	Yes	20.2	40.6	20.34
8	M	28	CD	+++	+++	A + C	A + C	Terminal ileum	Yes	17.7	41.7	24.01
9	M	37	CD	++	+	C	C	Terminal ileum	No	23.2	27.6	4.39
10	M	48	CD	++	++	C	C	Terminal ileum	No	25.6	36.6	11.05
11	M	45	CD	++	+++	A + C	A + C	Terminal ileum	Yes	27.1	38.7	11.63
12	M	24	CD	++	++	A + C	A + C	Terminal ileum	Yes	26.5	37.4	10.92
13	F	18	CD	+++	++	A	A	Terminal ileum	Yes	17.3	22.9	5.6
14	F	37	CD	++	+	C	A + C	Terminal ileum	Yes	27.2	32.0	4.72
15	F	48	CD	+	+	A + C	A + C	Terminal ileum	No	23.7	N/A	/
16	M	46	s. CD	–	–	–	–	N/A	No	25.1	N/A	/
17	F	52	CD	++	+	C	C	Sigma/rectum	No	27.8	39.1	11.31
18	F	55	CD	–	–	–	–	N/A	No	25.5	N/A	/
19	M	29	CD	+++	+++	A + C	A + C	Ileum	Yes	30.9	38.1	7.21
20	F	66	CD	++	+	C	C	Ileum	Yes	31.5	28.7	2.77
21	M	73	s. CD	–	–	–	–	N/A	No	25.2	N/A	/
22	M	47	CD	++	++	C	C	Colon	No	23	33.1	10.15
23	M	30	CD	++	++	A + C	A + C	Terminal ileum	Yes	26.2	34.5	8.27
24	M	31	CD	+++	+++	C	A + C	Terminal ileum	Yes	28.6	33.4	4.82
25	F	39	CD	–	–	–	–	N/A	No	23.7	N/A	/
26	M	47	CD	–	–	–	–	N/A	No	N/A	N/A	/
27	F	35	CD	++	++	A + C	A + C	Terminal ileum	Yes	29.2	38.0	8.83
28	M	56	CD	+	+	A + C	C	Terminal ileum	Yes	26.3	38.5	12.2
29	M	34	CD	++	++	C	A + C	Sigma/rectum	Yes	25.7	32.5	6.8
30	M	26	CD	++	++	A	A	Terminal ileum	Yes	24.8	25.0	0.2
31	M	29	CD	+	+	A + C	A + C	Terminal ileum	Yes	26.5	34.7	8.2

Diagnosis: Crohn's disease (CD), suspected CD (s. CD), Cytomegalovirus (CMV), indeterminate collitis (IC); Clinical activity: "−"no disease activity, "+" low activity, "++" moderate activity, "+++" high activity; Disease state: "A" acute and active inflammatory disease state, "C" chronic fibrostenotic disease state, "A + C" transitional forms with both acute- and chronic-fibrotic changes possibly with fistula and stenosis. Magnetization transfer ratio of morphologically normal bowel wall (MTR-n) and of pathologically altered bowel wall (MTR-p) as well as the difference between these values if provided. Reader one (R1); reader two (R2); "*" patients with 3D magnetization transfer gradient-echo sequence

fat-suppressed 3D gradient-echo sequences and an axial T1-weighted 2D gradient-echo sequence with water selective excitation were acquired.

Data evaluation

The magnetization transfer ratio (MTR) is a quantitative measure of the interaction between the low and high-mobility proton pools in a given tissue, as assessed with a given acquisition. MTR is defined as [3]

$$\mathrm{MTR} = \frac{\mathrm{SI}_0 - \mathrm{SI}_{\mathrm{SAT}}}{\mathrm{SI}_0}$$

where SI_0 and $\mathrm{SI}_{\mathrm{SAT}}$ refer to the image intensity without and with the saturation prepulse, respectively. From the data sets, the MTR values were calculated pixelwise with custom-made computer scripts written in the programming language Matlab (The Mathworks, Inc., Natick, MA). In the, thus, obtained MTR maps, the MTR was quantified by region-of-interest (ROI) analysis. MTR values were determined for skeletal muscle, cartilage tissue, renal

Table 2 MRI sequence parameters

MRI sequence parameters							
Parameter	T2w FSE ax	T2w FSE cor	SSFP cor	MT GRE ax	MT GRE ax	T1w GRE cor	T1w GRE ax
Encoding	2D	2D	2D	2D	3D	3D	2D
Field-of-view (mm)	300 × 227	400 × 400	400 × 376	395 × 282	380 × 302	400 × 400	375 × 309
Image matrix	248 × 187	248 × 220	268 × 266	196 × 141	252 × 201	204 × 201	204 × 139
Slice thickness (mm)	4	7	4	4	4	4	7
Intersection spacing (mm)	4.4	1	3	0	0	0	1
Voxel size (mm)	1.2 × 1.2	1.6 × 1.8	1.5 × 1.5	2.0 × 2.0	1.5 × 1.5	2.0 × 2.0	1.8 × 2.2
Echo time (ms)	80	80	2.1	2.2	4.6	2	4.9
Echo train length/TFE factor	67	78	132	–	–	47	–
Repetition time (m)	459.8	444.2	4.2	32	32	4.3	259.3
Flip angle (°)	90	90	90	25	15	10	70
Averages	1	2	1	1	2	2	2
Bandwidth (Hz/px)	760.8	677.7	1275.7	385.1	161.3	375.6	351.4
No. of slices	46	25	34	10	50	75	50
Fat suppression	SPAIR	SPAIR	No	No	No	SPAIR	ProSet
Respiratory control	BH	BH	BH	BH	Free B	BH	BH
Acquisition time	0:21	0:11	0:19	0:25	2:40	0:21	0:32

Ax axial, *Cor* coronal, *FSE* fast spin echo, *SSFP* steady state free precession, *MT* magnetization transfer, *GRE* gradient-echo, *BH* breath hold, free B free breathing, SPAIR spectral selection attenuated inversion recovery, *ProSet* principle of selective excitation technique

cortex and liver parenchyma as a reference, as well as from non-affected small bowel and from pathologically altered bowel structures, which were identified in the standard imaging protocols. At least 4 ROIs were positioned for each tissue. Mean MTR were obtained by averaging all ROI measurements from each tissue and each patient. Great care was taken to avoid partial volume effects. The ROIs were defined freeform in areas in which the bowel wall could clearly be identified. Bowel segments with insufficient distension or with intraluminal food debris were excluded from the analysis. ROI sizes were typically between 12 and 50 mm^2 for the non-affected small bowel wall, between 25 and 100 mm^2 for the pathologically altered bowel and between 68 and 500 mm^2 for the reference tissues. All ROI measurements in the MTR maps were made by the same author (S.P. with more than 3 years of experience in MR imaging).

Clinical grading

All patients with pathologically altered bowel were classified in different disease states by two independent readers (A.B. and N.C., with 9 and 4 years of experience in abdominal MRI, respectively) based on previously described classifications [6–8]. "A" acute and active inflammatory disease state; "C" chronic fibrostenotic disease state and "A + C" transitional forms with both acute- and chronic-fibrotic changes possibly with fistula and stenosis (Table 3). To distinguish between acute- and chronic-fibrotic disease as well as between stenosis due to acute inflammation or due to fibrosis, the readers used all acquired MRI sequences and available histological findings ($n = 13$). "A" acute and active inflammatory disease state was defined as an acute inflammation of the bowel wall (bowel wall thickening >3 mm) with nodular, polypoid or asymmetric intestinal thickening, high mural signal intensity on T2w fat-saturated images, layered pattern of enhancement, imbibition of the surrounding fat tissue and histological findings with signs of an acute inflammation. "C" chronic fibrostenotic disease state was assigned in patients with stricturing disease behavior, bowel obstruction due to fibrotic-stenotic changes, fixed narrowing of the affected segment with hypointense signal in T1w and T2w sequences, inhomogeneous contrast enhancement and no evidence of edema or surrounding mesenteric inflammation [6–8]. If the findings showed criteria for both disease states "A" and "C," then the readers assigned these patients as transitional forms "A + C". Moreover, all patients were classified in a clinical score-scale for determination of the clinical activity at the time of the MR examination (Table 3). Based on a previously described classification of CD activity [9], we divided the patients in 4 different stage-related groups: "−"no disease activity; "+" low activity; "++" moderate activity; "+++" high activity. For grading of the disease activity, all available clinical data from the patient records were used such as weight loss, clinical symptoms at presentation, CRP (C-reactive Protein) values in the blood serum and fecal calprotectin

values. Furthermore, typical patterns of disease activity as found in the standard MRI data sets were considered as well (such as bowel wall thickening, mucosal or submucosal edema, imbibition of the surrounding fat tissue, lymph node enlargement, pattern and degree of contrast-medium uptake as well as bowel obstruction or abscess).

Statistical evaluation

Reader agreement was assessed by Cohen's kappa coefficient. Kappa values of 0.01–0.4 were considered to indicate slight or fair agreement, 0.41–0.6 moderate agreement, 0.61–0.8 substantial agreement and values higher than 0.81 almost perfect agreement [10]. Other results are reported as mean ± standard deviation. The data was descriptively reviewed and statistically tested for normality with the Kolmogorov–Smirnov test. P values were calculated by using the Student's *t* test for paired samples. A p value <0.05 was considered significant. All statistical analyses were performed using commercially available software (SPSS, version 19.0, Chicago, IL, USA). For the estimation of the optimal cutoff of the MTR values for detection of bowel fibrosis, we used a receiver operating characteristic (ROC) curve [11]. The optimal cutoff was defined as the value at which the sum of the sensitivity and specificity was maximized.

Results

Grading of the patients with clinical findings/ conventional MR enterography

Five of the 31 included patients had completely normal MR findings of the small and large bowel. The remaining 26 patients presented pathological imaging features typical of chronic inflammatory bowel disease. Three of these patients showed acute inflammation of the bowel wall (Table 1, patient 5, 13 and 30). Patient five was simultaneously affected by Cytomegalovirus associated colitis. The other 23 patients had chronic-fibrotic inflammation with or without an additional feature of acute disease. Reader one assigned ten patients to the chronic-fibrotic disease state, and 13 to the group with additional acute inflammation. The second reader ranked eight and 15 in the respective groups. The reader agreement was almost perfect (κ value of 0.81). In four patients (Table 1, patient 14, 24, 28 and 29), the reader classification showed a discrepancy. In consensus reading, these patients were considered to have both acute and chronic-fibrotic changes, as one of the readers detected characteristics for both disease states. From the 26 patients with pathological bowel alterations, five had changes of the colon (including sigma

Table 3 Criteria of the clinical activity score and for distinction between acute inflammatory stenosis and chronic-fibrotic stricture

Score	Characteristic findings
–	No pathologic bowel segments in MRI; no inflammatory parameters; constant body weight
+	Pathologically altered bowel segments in MRI; no inflammatory parameters; good therapy response
++	Pathologically altered bowel segments; fistula; moderate increase in inflammatory parameters; weight loss
+++	Abscess or obstruction; fistula; lymphadenopathy; marked increase in inflammatory parameters; weight loss or/and underweight; temperature; abdominal pain; reduced appetite
Disease state	Pathological MRI findings
Acute/active inflammatory disease	Acute inflammation, bowel wall thickening >3 mm; nodular, polypoid or asymmetric intestinal thickening; high mural signal intensity on T2w fat-saturated images; layered pattern of enhancement; imbibition of the surrounding fat tissue; histological findings with signs of an acute inflammation
Chronic fibrostenotic disease	Stricturing behavior; bowel obstruction due to fibrotic-stenotic changes; fixed narrowing of the affected segment with hypointense signal in T1w and T2w sequences; inhomogeneous contrast enhancement; no evidence of edema or surrounding mesenteric inflammation

Criteria to graduate the clinical activity of Crohn's disease and typical MR findings to distinguish acute inflammation from chronic-fibrotic alterations [6–9]

and rectum) (Table 1, patient 3, 5, 17, 22 and 29). In the other 21 patients, the small intestine was affected (predominantly the terminal ileum; $n = 19$). One of the patients with chronic and acute inflammation of the colon was finally diagnosed with indeterminate colitis (Table 1, patient 3) instead CD, while all other patients had the diagnosis of CD. Stenosis or stricture of the bowel wall was found in the MR images of 18 patients.

From the 26 patients with pathological features, reader one assigned 6, 14 and 6 patients to the high, moderate and low disease activity groups, respectively. The second ranked 6, 10 and 10 patients in the respective groups. The inter-reader agreement was substantial with a κ value of 0.65.

Image quality of the MT sequences

The 3D gradient-echo sequence with an acquisition time of 2:40 min per data set, which we evaluated in the first four patients, showed strong magnetization transfer effects (Fig. 1a). Although the patients were asked for shallow breathing during the scan, significant motion artefacts could not be avoided. These artefacts hampered the quantitative analysis, particularly since they were more evident in the subtraction images for MT quantification. These patients were excluded from the quantitative data evaluation. The 2D MT sequence that we finally included in the MRE protocol was acquired during breath hold (acquisition time 25 s) and provided images free of breathing artefacts (Fig. 1b). The rather long acquisition time of 25 s was well tolerated by the young patient population. Furthermore, no relevant bowel movement artefacts were noted in the subtraction images. In contrast to the 3D sequence, minor opposed-phase artefacts were visible at the interface between bowel wall and peritoneal fat, which, however, did not hamper the image analysis. In all volunteers, image quality was sufficient to identify pathologically altered bowel segments if present, based on the conventional MRE protocol. The MTR map of only one of the patients (Table 1, patient 26) had to be excluded from quantitative analysis due to body movement between the two acquisitions.

Quantitative evaluation of MTR

In the quantitative evaluation of the 2D MT sequence, we measured high MTR values in reference tissues known to exhibit high MT: skeletal muscle tissue 49.9 ± 1.2 % ($n = 27$) (psoas muscle and the erector spinae muscle) and cartilage 62.3 ± 6.2 % ($n = 9$) (intervertebral disk). In the parenchyma of the abdominal organs, somewhat lower MTR values were measured: renal cortex 31.1 % ± 2.0; $n = 6$ and liver 38.7 %; $n = 1$. In the normal, unaffected bowel wall segments of the patients diagnosed with fibrosis based on the standard MRI protocol, a mean MTR of

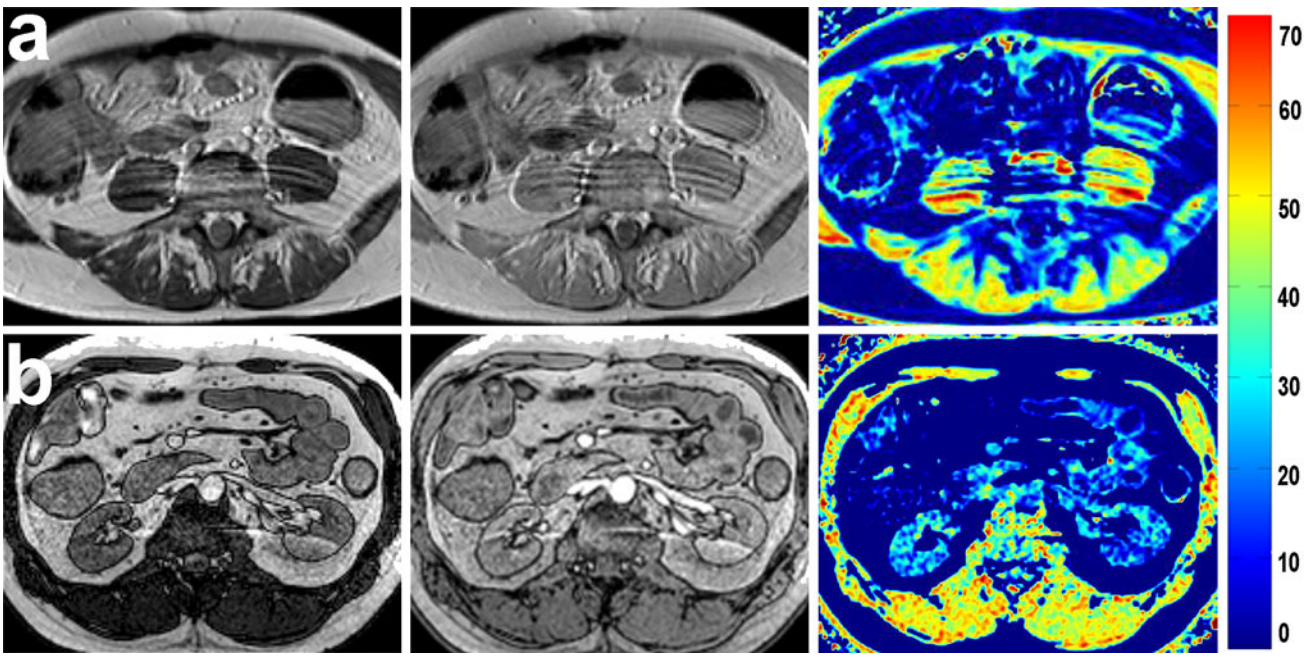

Fig. 1 Typical images acquired with the 3D and 2D encoding scheme are displayed, **a** data set with 3D encoding, **b** data set acquired with 2D encoding technique. *Left column* images acquired with MT prepulse, *middle column* without application of the MT prepulse, *right column* corresponding MTR map with a color scale in %. Comparing both acquisition schemes, it is clearly visible that the 3D data set exhibits stronger breathing artefacts compared to the 2D acquisition. The artefacts of the 3D encoding become even more pronounced in the MTR maps

Table 4 Magnetization transfer ratio of the measured bowel wall

Localization	Fibrosis	Normal bowel wall	Inflammation
MTR values (%)	35.3 ± 4.0	25.4 ± 3.4	22.9 ± 2.2
MTR (min/max) (%)	(27.6/41.7)	(17.3/31.5)	(20.7/25.0)
n	18	25	3
p	<0.0001	No significance	

Magnetization transfer ratio (MTR) as well as highest and lowest measured values in parentheses (MTR (min/max) of chronic-fibrotic bowel wall (*fibrosis*), of morphological *normal bowel wall* and of acute inflammation of the bowel wall (*inflammation*)

26.1 ± 3.4 % (range 17.7–31.5 %; $n = 18$) was measured. In contrast, the mean MTR in the fibrosed segments of the same patients was significantly higher with 35.3 ± 4.0 % (range 27.6–41.7 %; $n = 18$) ($p < 0.0001$) (Table 4; Fig. 2) with a mean paired difference of 9.7 ± 5.6 % (range 2.8–24.0 %). The mean MTR of bowel segments with acute inflammation was slightly lower (22.9 ± 2.2 %; range 20.7–25.0 %; $n = 3$) compared to healthy bowel wall structures (25.0 ± 3.7 %; range 17.3–31.5 %; $n = 25$) (Table 4; Figs. 2, 3). This difference was, however, not statistically significant ($p = 0.3$) (Fig. 4).

The measured MTR values of the bowel wall ($n = 46$; 25 non-altered bowel wall, 18 chronic-fibrotic segments and three acute inflamed segments) demonstrated sufficient power for identification of fibrotic segments (area under the ROC curve (AUC) 0.98 ± 0.01; 95 % CI). The optimal cutoff was at MTR = 28.7 % with a sensitivity of 95 % and a specificity of 90 %.

Discussion

Our study demonstrates that MT imaging of small bowel structures is feasible in a clinical setting with sufficiently high image quality for a quantitative assessment. Chronic-fibrotic strictures exhibited higher MTR compared to non-affected bowel wall. In contrast, in bowel segments with acute inflammatory stenosis, the MTR was similar to normal bowel wall or even slightly lower. To our knowledge, this is the first study that reports MT ratios for the bowel wall in human subjects affected by CD. The proposed technique might facilitate the differentiation of fibrotic strictures and acute inflammatory stenosis of the bowel wall in patients with CD, which has a strong impact on the treatment planning for these patients. Due to the short acquisition time of the 2D MT sequence, it can easily be implemented in a standard MRE protocol.

Our results are in excellent concordance with the findings of an animal study from Adler et al. [2], in which, for the first time, MT imaging was suggested for assessment of bowel wall fibrosis in CD. In this study, a relevant increase in the MTR (24.7 ± 1.9 %) in fibrotic segments of bowel wall in rats with PG-PS-induced intestinal fibrosis (a rat model of CD) was reported compared to a control group (10.8 ± 1.7 %) [2]. Adler et al. could demonstrate that the increase in MTR correlated with the grade of fibrosis (microscopically assessed as a histologic fibrosis score by two gastrointestinal pathologists blinded to the MR results) and with the amount of type I collagen, which was densitometrically measured. Since the MTR values depend on many data-acquisition parameters (such as the encoding mode (2D or 3D), the pre-saturation technique and parameters, the phase-encode order and corresponding k-space filling, the voxel size, the field strength, etc.) the results from Adler et al. could not quantitatively be compared with the results of our study.

We measured the MTR in pathologically altered bowel wall of patients with CD and compared them in an intra-individual comparison with mean MTR values in normal bowel segments. All imaging parameters (such as field-of-view, matrix size and repetition time) were kept constant to standardize the MT protocol as far as possible. The MTR values of different MT sequences cannot directly be compared, however, if all sequence parameters are kept constant the MT ratios are a quantitative measure appropriate for meaningful inter-individual comparisons.

A higher MTR value implies a larger amount of magnetization exchanged between the proton pools of low and high mobility in a tissue, due to, for example, a higher overall rate of exchange or to a larger pool of low-mobility protons. Possible explanations for our findings are (1) an increase in the concentration of collagen fibers in fibrotic tissue, like collagen type I, which was shown in the animal study from Adler et al. and which is known to bind a large number of water molecules or (2) a hyperplasia of the muscularis externa, which was also diagnosed in the animal study of Adler et al. in the fibrotic rat models and which may also lead to higher MTR values. The data in our current study do not provide a basis for an estimate of the relative weights of these potential mechanisms to the observed increase in the MTR values in the pathologically fibrotic bowel segments.

The transverse magnetization in the low-mobility proton pool relaxes rapidly with short time constants in the order of ~100 μs or even shorter, which results in homogeneously broadened resonance lines with widths of thousands of Hertz. It is thus possible to selectively saturate the system of the low-mobility proton pool. As a consequence, polarization and magnetization will be transferred to the pool of highly mobile protons, which dominantly contributes to the signal observed with standard medical imaging

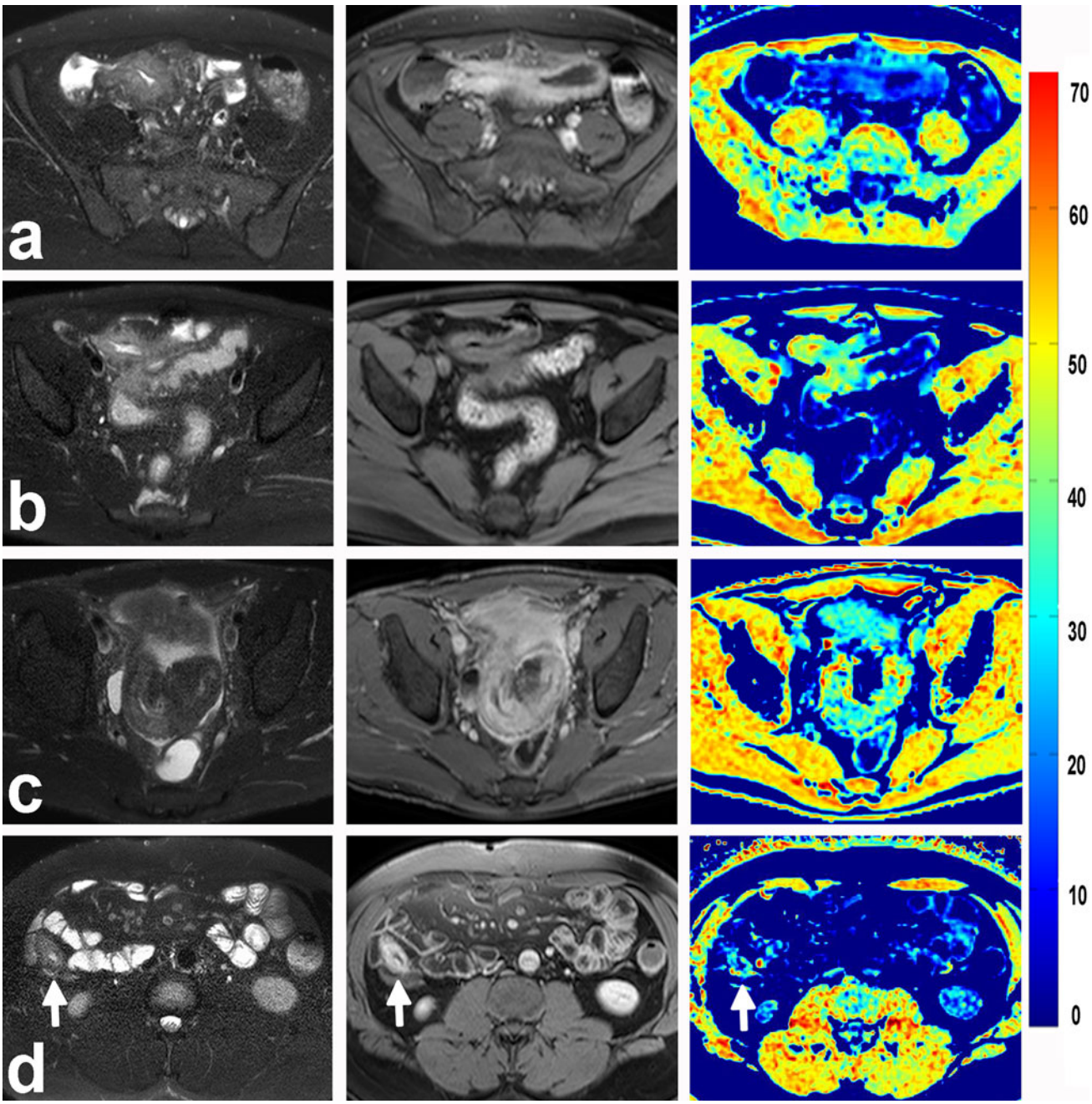

Fig. 2 T2w fat-saturated FSE images (*left column*), contrast-enhanced T1w fat-saturated GRE images (*middle column*) and parametrical MTR maps of the examined patients with Crohn's disease (*right column*); **a** a female, 18-year-old patient with acute inflammation of the bowel wall in the terminal ileum with mucosal and submucosal edema as well as imbibition of the surrounding fat tissue (active inflammatory disease); MTR map shows little magnetization transfer in the inflammatory bowel wall; **b** a male, 29-year-old patient with acute stenosis of the bowel lumen due to mucosal edema in addition to a chronic-fibrotic stricture of the terminal Ileum with internal fistula exhibiting high MT (chronic + acute ulcerative regional enteritis; fistula forming and perforating disease); **c** a male, 45-year-old patient with chronic stenosis and stricture in the terminal Ileum showing high MT in the affected bowel segment (fibrostenotic disease); **d** a male, 37-years-old patient with focal thickening of the bowel wall in the terminal ileum with corresponding contrast enhancement (*arrows*) as well as normal bowel loops. MTR values are notably higher in segments with chronic-fibrotic changes compared to the morphologically normal bowel structures. Color scale in %

sequences, from the low-mobility pool, and, thus, the observed signal will decrease. The transfer occurs with rates that are in the range of the T1 relaxation times in the low-mobility proton pool, and the effects only build up over time periods that are not negligibly short when compared with, for example, TR times. For quantitative assessments of MTR with gradient-echo sequences and pre-saturation pulses, this means that the sequence design

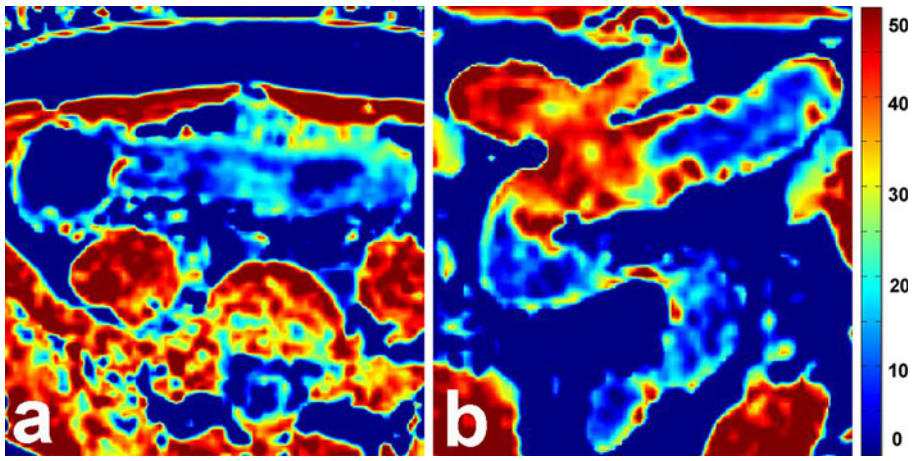

Fig. 3 Parametrical MTR maps of the first two patients from Fig. 2 with a smaller color map range (0–50 %) showing in more detail the focal MTR changes within the bowel; **a** the magnetization transfer in the inflammatory bowel wall approximately corresponds to a value between 18 and 23 %, whereas the chronic-fibrotic stricture in **b** shows higher MTR ranges between 35 and 50 %

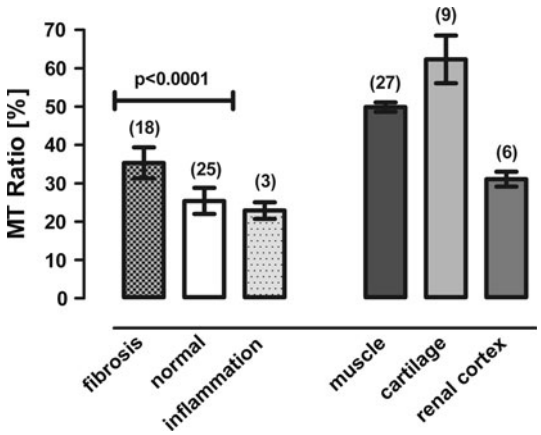

Fig. 4 Magnetization transfer ratio in % of chronic-fibrotic bowel wall (*fibrosis*), of morphologically normal bowel wall (*normal*) and of acute inflamed bowel wall (*inflammation*) as well as of further reference tissues (*muscle, cartilage and renal cortex*); number of patients in *parentheses* above the corresponding *bars*

needs to be optimized in a trade-off between the magnitude of the observed MT effects and the acquisition time. Typically, carefully tailored 3D sequences with interleaved saturation and imaging pulses have been found to offer a better SNR for MTR assessments than competitive 2D sequences. Unfortunately, the acquisition time of the 3D sequences is in general too long to fit into a single breath hold. In our study, we found 3D acquisitions during constant shallow breathing to result in image artefacts that were too severe to allow a meaningful quantitative assessment of MTR values. In addition, the 3D sequence could not be combined with synchronization techniques such as triggering based on navigator or breathing-belt data.

To avoid the breathing artefacts, we resorted to a multi-slice 2D sequence with a lower number of encoding steps and slice-selective spin excitation. The slice-selective spin excitation pulses also act as off-resonance prepulses in other imaging slices of the same interleaved acquisition, thereby causing an increased saturation of the macromolecular pool even in the sequence acquired without the MT prepulse. Therefore, a lower MTR is expected to be obtained from the corresponding images when compared with those from the 3D acquisition. To sufficiently accelerate the 2D acquisition, we also had to increase the receiving bandwidth and to use parallel encoding techniques, which resulted in lower signal-to-noise ratio compared to the 3D sequence. However, we were able to show that in spite of the disadvantageous parameter changes, image quality was sufficiently high and the magnetization effects were large enough for a quantitative assessment of the MTR in small bowel segments. The observed MTR values were in good agreement to previously reported data for reference tissues such as skeletal muscle, cartilage tissue or renal cortex [12–14]. The normalization of the MTR values to a reference tissue might be suitable to reduce unwanted signal variations in further studies. Minor opposed-phase artefacts were visible in the images from the 2D MT sequence due to a shortening of the echo time to 2.1 ms, which we tolerated for the benefit of an increased signal-to-noise ratio. The effect might be minimized using fat saturation.

Our study has the following limitations:

1. The majority of patients, typical for patients undergoing MRE imaging, were in the chronic phase of the disease and showed fibrostenotic segments with a more or less pronounced additional inflammation. We had a relatively small number of patients with “pure” acute inflammation or “pure” fibrosis.
2. Histopathological confirmation was not routinely obtained. It would have been difficult to justify an additional invasive procedure for research purposes in this patient cohort that already underwent a great number of clinical examinations during the course of their disease. On the other hand, MRE is intended to

avoid ileocolonoscopy in a clinical setting. It was previously shown that MRE may serve as an alternative to endoscopy in the evaluation of the activity of ileocolic CD with sufficient sensitivity and specificity for assessment of bowel wall thickening, mucosal or submucosal edema, imbibition of the surrounding fat tissue and lymph node enlargement [7, 15–19]. A combination of clinical symptoms; endoscopic, radiological, histopathological and surgical findings as well as laboratory parameters are taken into account for diagnosis and therapy monitoring in CD [20]. We have considered the revised Montreal classification of CD [6] as well as the classification from Maglinte et al. [8] to evaluate the current activity of the disease. Similar to disease activity, the presence of fibrosis was not histologically confirmed in all patients, but was assessed based on imaging features in combination to the clinical findings.

3. In our study, we did not evaluate if the additional information from MT imaging would have altered patient management, treatment decisions or outcome. The aim of our study was to gain initial experience with MT imaging of the bowel wall in humans and its potential application in the assessment of bowel wall fibrosis in CD. Future prospective studies should be sought that include an assessment of patient outcome depending on the additional diagnostic information available from MT imaging in the MRE protocols of small bowel.
4. No algorithm for image registration of the sequences with and without MT pulse was applied. However, the reproducibility of the bowel position between the two subsequent sequences seemed high as we did not find relevant motion artefacts in the MTR maps, potentially due to the smaller bowel movement in patients with CD compared to healthy subjects.
5. The chosen 2D MT sequence does not cover the entire abdomen, but approximately 40–50 % in the craniocaudal direction. In this study, a radiologist was present during the MR measurement to determine area of affected bowel structures for planning of the MT sequences. For coverage of the complete abdomen, both, the sequence with MT preparation and the sequence without MT preparation need to be applied 2–3 times each.

Conclusion

In conclusion, we demonstrated that MT can be measured in the human bowel wall using a 2D encoded gradient-echo sequence with a MT prepulse; the proposed quantitative technique can contribute to the differentiation of fibrotic strictures from acute inflammatory stenosis of the bowel wall in patients with CD at the expense of only a few minutes additional examination time.

References

1. Rieber A, Aschoff A, Nüssle K et al (2000) MRI in the diagnosis of small bowel disease: use of positive and negative oral contrast media in combination with enteroclysis. Eur Radiol 10:1377–1382
2. Adler J, Swanson SD, Schmiedlin-Ren P, Higgins PD, Golembeski CP, Polydorides AD, McKenna BJ, Hussain HK, Verrot TM, Zimmermann EM (2011) Magnetization transfer helps detect intestinal fibrosis in an animal model of Crohn disease. Radiology 259(1):127–135
3. Henkelman RM, Stanisz GJ, Graham SJ (2001) Magnetization transfer in MRI: a review. NMR Biomed 14(2):57–64
4. Schunk K, Metzmann U, Kersjes W, Schadmand-Fischer S, Kreitner KF, Duchmann R, Protzer U, Wanitschke R, Thelen M (1997) Follow-up of Crohn's disease: can hydro-MRI replace fractionated gastrointestinal passage examination? Rofo 166(5):389–396
5. Schunk K, Kern A, Oberholzer K, Kalden P, Mayer I, Orth T, Wanitschke R (2000) Hydro-MRI in Crohn's disease: appraisal of disease activity. Invest Radiol 35(7):431–437
6. Silverberg MS, Satsangi J, Ahmad T et al (2005) Toward an integrated clinical, molecular and serological classification of inflammatory bowel disease: Report of a Working Party of the 2005 Montreal World Congress of Gastroenterology. Can J Gastroenterol 19(Suppl A):5–36
7. Punwani S, Rodriguez-Justo M, Bainbridge A, Greenhalgh R, De Vita E, Bloom S, Cohen R, Windsor A, Obichere A, Hansmann A, Novelli M, Halligan S, Taylor SA (2009) Mural inflammation in Crohn disease: location-matched histologic validation of MR imaging features. Radiology 252(3):712–720
8. Maglinte DD, Gourtsoyiannis N, Rex D, Howard TJ, Kelvin FM (2003) Classification of small bowel Crohn's subtypes based on multimodality imaging. Radiol Clin North Am 41:285–303
9. Harvey RF, Bradshaw JM (1980) A simple index of Crohn's-disease activity. Lancet 1(8167):514
10. Landis JR, Koch GG (1977) The measurement of observer agreement for categorical data. Biometrics 33(1):159–174
11. Hanley JA, McNeil BJ (1982) The meaning and use of the area under the receiver operating characteristic (ROC) curve. Radiology 143:29–36
12. Boss A, Martirosian P, Küper K, Fierlbeck G, Claussen CD, Schick F (2006) Whole-body magnetization transfer contrast imaging. J Magn Reson Imaging 24(5):1183–1187
13. Stanisz GJ, Odrobina EE, Pun J, Escaravage M, Graham SJ, Bronskill MJ, Henkelman RM (2005) T1, T2 relaxation and magnetization transfer in tissue at 3T. Magn Reson Med 54(3):507–512
14. Li JG, Graham SJ, Henkelman RM (1997) A flexible magnetization transfer line shape derived from tissue experimental data. Magn Reson Med 37(6):866–871
15. Schreyer AG, Rath HC, Kikinis R, Völk M, Schölmerich J, Feuerbach S, Rogler G, Seitz J, Herfarth H (2005) Comparison of magnetic resonance imaging colonography with conventional colonoscopy for the assessment of intestinal inflammation in patients with inflammatory bowel disease: a feasibility study. Gut 54(2):250–256
16. Taylor SA, Punwani S, Rodriguez-Justo M, Bainbridge A, Greenhalgh R, De Vita E, Forbes A, Cohen R, Windsor A,

Obichere A, Hansmann A, Rajan J, Novelli M, Halligan S (2009) Mural Crohn disease: correlation of dynamic contrast-enhanced MR imaging findings with angiogenesis and inflammation at histologic examination–pilot study. Radiology 251(2):369–379

17. Rimola J, Rodriguez S, García-Bosch O, Ordás I, Ayala E, Aceituno M, Pellisé M, Ayuso C, Ricart E, Donoso L, Panés J (2009) Magnetic resonance for assessment of disease activity and severity in ileocolonic Crohn's disease. Gut 58(8):1113–1120
18. Horsthuis K, Bipat S, Bennink RJ, Stoker J (2008) Inflammatory bowel disease diagnosed with US, MR, scintigraphy, and CT: meta-analysis of prospective studies. Radiology 247:64–79
19. Gourtsoyiannis N, Grammatikakis J, Papamastorakis G et al (2006) Imaging of small intestinal Crohn's disease: comparison between MR enteroclysis and conventional enteroclysis. Eur Radiol 16:1915–1925
20. Stange EF, Travis SP, Vermeire S et al (2006) European Crohn's and Colitis Organisation. European evidence-based consensus on the diagnosis and management of Crohn's disease: definitions and diagnosis. Gut 55(suppl 1):i1–i15